Chemically exfoliating large sheets of phosphorene via choline chloride urea viscosity-tuning

2017 Nanotechnology 28 155601

(http://iopscience.iop.org/0957-4484/28/15/155601)

IOP Publishing Nanotechnology
Nanotechnology 28 (2017) 155601 (6pp) https://doi.org/10.1088/1361-6528/aa62f6

Chemically exfoliating large sheets of phosphorene via choline chloride urea viscosity-tuning

A Ng[1], T E Sutto[2], B R Matis[3], Y Deng[4], P D Ye[4], R M Stroud[2], T H Brintlinger[2] and N D Bassim[2,5]

[1] NRC Postdoctoral Scholar, US Naval Research Laboratory, Washington, District of Columbia, 20375, United States of America
[2] Materials Science and Technology Division, US Naval Research Laboratory, Washington, District of Columbia, 20375, United States of America
[3] Acoustics Division, US Naval Research Laboratory, Washington, District of Columbia, 20375, United States of America
[4] School of Electrical and Computer Engineering, Purdue University, West Lafayette, Indiana, 47907, United States of America

E-mail: amy.ng.ctr@us.af.mil

Received 11 November 2016, revised 7 February 2017
Accepted for publication 24 February 2017
Published 16 March 2017

Abstract

Exfoliation of two-dimensional phosphorene from bulk black phosphorous through chemical means is demonstrated where the solvent system of choice (choline chloride urea diluted with ethanol) has the ability to successfully exfoliate large-area multi-layer phosphorene sheets and further protect the flakes from ambient degradation. The intercalant solvent molecules, aided by low-powered sonication, diffuse between the layers of the bulk black phosphorus, allowing for the exfoliation of the multi-layer phosphorene through breaking of the interlayer van der Waals bonds. Through viscosity tuning, the optimal parameters (1:1 ratio between the intercalant and the diluting solvent) at which the exfoliation takes place is determined. Our exfoliation technique is shown to produce multi-layer phosphorene flakes with surface areas greater than 3 μm^2 (a factor of three larger than what has previously been reported for a similar exfoliation method) while limiting exposure to the ambient environment, thereby protecting the flakes from degradation. Characterization techniques such as optical microscopy, Raman spectroscopy, ultraviolet–visible spectroscopy, and (scanning) transmission electron microscopy are used to investigate the quality, quantity, and thickness of the exfoliated flakes.

Supplementary material for this article is available online

Keywords: phosphorene, choline chloride urea, chemical exfoliation

(Some figures may appear in colour only in the online journal)

1. Introduction

Beginning with the discovery of graphene, two-dimensional (2D) materials have become a topic of interest in numerous fields of science, due to a variety of unique physical, electrical and optical properties, which arise from their inherently 2D nature [1]. While graphene remains intensely studied, other 2D materials have gained attention owing to their potential use in novel device applications in addition to being suitable platforms for carrying out basic research; for example, these materials include hexagonal boron nitride (h-BN), an insulating, hyperbolic metamaterial [2, 3]; transition metal dichalcogenides (TMDs) like molybdenum disulfide (MoS_2)

[5] Current affiliation: Department of Materials Science and Engineering, McMaster University, Hamilton, Ontario, L9H 4L7, Canada.

whose electronic transport can range from insulating to metallic [4, 5]; and germanene, another Group-IV elemental allotrope with similarities to grapheme [6]. In this work, we focus on phosphorene, the 2D version of black phosphorus (BP) that has been shown to have useful electronic properties including a room temperature mobility of 286 $cm^2\ V^{-1}\ s^{-1}$ and a nonzero band gap of 1.88 eV, which are promising for logic operations [7, 8]. Despite the technological promise that BP-derived materials possess, there are factors hindering their development, including an instability in ambient air and the difficulty of obtaining large-area films with controllable thickness. Thus, phosphorene production techniques that can yield large-area, thin flakes while at the same time minimize or delay the onset of environmental degradation are greatly desired. While chemical vapor deposition (CVD) growth processes are an option that can potentially solve the scalability problem, CVD of phosphorene is currently a nascent field of research, and has not been shown to minimize ambient exposure, which leaves chemical or mechanical exfoliation as the primary means of obtaining BP-derived 2D materials [9, 10]. Chemical exfoliation is a promising candidate for obtaining phosphorene since it is a material production method that can be compatible with device technologies and might limit ambient exposure due to chemical encapsulation [11–14]. Therefore, gaining insight into the contributing processes to the chemical exfoliation of phosphorene from the bulk, and how such a method can simultaneously serve to protect the material from degradation, will aid in its adoption for various applications, such as the fabrication of optical sensors and field-effect transistors.

Chemical exfoliation, an alternative to the conventional 'scotch-tape' or mechanical method, relies on the ability of a solvent molecule to intercalate between adjacent layers of a solid to decrease the local van der Waals bonds between them. Chemical exfoliation has been shown to have a higher yield at a faster rate than mechanical exfoliation, which relies on an externally-bonded adhesive and a globally applied mechanical force to overcome the local van der Waals bonds [15]. Furthermore, successful choice of solvent can impact its overall yield where prior studies have shown enhanced chemical exfoliation by matching surface tensions of the solvents to the surface energies of the bulk material [16, 17]. One class of solvents that provides flexibility in this, and other parameters, is ionic liquids (ILs), which have already been used to intercalate graphite and other potential low-dimensional materials, the first step in chemical exfoliation [18, 19]. Moreover, a similar approach was applied to BP to obtain phosphorene flakes; however, they proved to be too small ($<1\ \mu m^2$) for many devices and applications, due to the high powered sonication resulting in nanosheets [20].

We present results on the chemical exfoliation of BP via a carbamide-based deep eutectic solvent (DES), a solvent type similar to an IL, except without complete charge separation (anion and cation species), found, for example, in imidazolium-based ILs. Instead, these compounds rely on weak hydrogen bonding between an electron donor and acceptor for stability; the weak hydrogen bonding in DESs allow for a surface tension better matching the surface energy of the bulk material. Because DES systems can be designed with a wide variety of organic acids and bases, solvent properties such as hydrophobicity, hydrophilicity, surface tension, viscosity and surface chemistry interactions can be controllably varied, which is necessary for optimizing the exfoliation process for different materials and achieving control over film thickness. Previously, these unique properties of DES systems were used to obtain graphene from graphene oxide [21]. Yet, little work has been done appropriating DES systems for chemical exfoliation of BP, and the influence of a DES on BP degradation has not been addressed. Using a high viscosity DES, bulk BP can be suspended as flakes after agitation; moreover, high surface tension in the DES influences the ability to exfoliate single sheets according to Kang *et al* by closely matching the high surface energy of the bulk BP to the surface tension of the solvent [17]. Similarly, the intercalation of ILs between the individual layers of a van der Waals bonded bulk material is believed to be the driving force for IL-based exfoliation, as well as a lesser investigated point that DESs/ILs form a barrier between ambient air and the air-sensitive flake [22]. All this notwithstanding, our study investigates the role a DES plays in the isolation of single- or few-layer sheets of phosphorene as well as the conditions for successfully implementing such a process, i.e. optimal viscosity.

2. Methods

The synthesis of our chosen DES, choline chloride-urea (CCU), is as follows: 139.6 grams of choline chloride (Sigma Aldrich 98%) was placed in a 500 ml round-bottom flask with a large magnetic stir bar. Then, 30.0 grams of urea or carbamide (Sigma Aldrich, BioReagent grade) is slowly added while stirring (2:1 molar ratio of choline chloride to urea) producing a slightly yellow-colored liquid after all of the urea was added. Finally, the CCU was heated to 40 °C and dried for 12 h under a dynamic vacuum (pressure, $P \sim 10^{-3}$ Torr). A more detailed procedure can be found elsewhere [23].

Bulk BP was crushed with mortar and pestle to obtain small pieces which were then submerged into a 2 dram vial filled with ~0.25 ml of CCU diluted with ethanol. In our experiments we systematically changed the volumetric ratio of CCU to ethanol in order to controllably alter the viscosity of the solvent system. The viscosities ranged from 8.0 centipoise to 190 centipoise (a function of the CCU to ethanol ratio), were quantified using a Cambridge ViscoLab 4000 viscometer, and were modulated to determine the optimal conditions for the exfoliation. (The viscometer was equipped with a Julabo F12 circulating temperature bath, where measurements were made approximately every 5 °C after 5 min of equilibrating at the set temperature. In continuous operating mode, the value for each temperature was taken after 3 successive viscosity measurements showed an error of less than 0.25%.) Diluting the DES with ethanol further minimizes the sample exposure to the DES, which reduces the possibility of an undesired reaction between the CCU and the BP. The vial was then sonicated in a water bath at 20 W for 120 min. Mechanical agitation is typically performed in chemical

exfoliation experiments to hasten the intercalation since unaided diffusion of the intercalating species is a slow process, where the input power used in prior work has exceeded 80 W; additionally, most intercalation reactions require increased heat to allow for a more 'fluid' solvent [24, 25]. However, due to the reactivity of BP, for our experiments low-powered, room temperature mechanical agitation is selected as a means of increasing the speed of the intercalation of the CCU between the layers of bulk BP, while minimizing heat. The resulting suspension was allowed to rest for approximately one minute before it was drop-cast onto a TEM grid (SPI lacey carbon) for obtaining atomic-scale images or a 275 nm SiO_2/Si (1 cm × 1 cm) wafer for optical and Raman spectroscopy characterization. In order to remove residual CCU, the TEM grids were soaked in pure ethanol for 1.5 days and the SiO_2 wafers were rinsed with an excess of ethanol. As a control experiment, the same process described above was performed with pure ethanol. In order to determine whether or not the DES can serve as a protective layer for the exfoliated phosphorene, Raman measurements were performed at two separate times using the same sample after the BP flakes were cast onto the substrate: immediately after the drop casting and 24 h later. Using optical microscopy and UV–vis spectroscopy, the number of flakes was quantified as well as their general sizes. Flake thickness was determined using Raman spectroscopy.

3. Results and discussion

Figure 1(a) summarizes the counting and size statistics of the exfoliated flakes for each CCU:ethanol mixture over a 1 cm × 1 cm area. We find that the number of flakes increases with increasing CCU concentration with local maxima at 20% and 60% while flakes with the largest areas were found for a CCU concentration of 50%. Overall, these results suggest that the ability to produce large, thin exfoliated sheets of phosphorene is dependent upon three key parameters: (1) the concentration of CCU in the CCU:ethanol mixture, (2) the viscosity of the solution, and (3) degree of intercalation. In terms of the number of sheets, we see an increase in the 20% CCU solution, which then decreases again for the 40% and 50% solutions. We attribute this behavior to the degree of intercalation of the solvent (i.e. edge only intercalation versus a more complete intercalation). As we vary the CCU from pure ethanol to the 20% solution, it is likely that the CCU is able to intercalate the BP. The very low viscosity of the 20% solution (8.4 cP) would allow for rapid diffusion into the BP, but with a large excess of ethanol (a molecule that is known to have weak interactions with the BP), it is likely that the limited CCU is not effective enough to delaminate the bulk material [26]. Thus, it is because of the edge-only intercalation that sheet area remains relatively small for the 20% and 40% solutions. However, for the 50% CCU solution (71.1 cP), the higher amount of CCU allows for a deeper penetration into the van der Waals gap of BP, and the optimized balance between viscosity and intercalant results in increased exfoliation and suspension in solution.

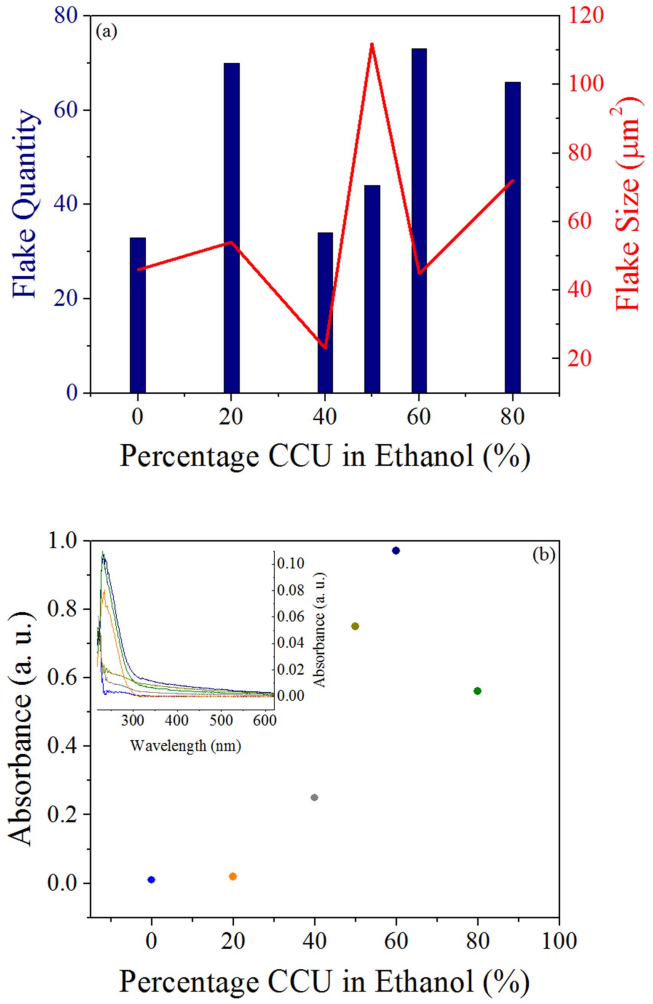

Figure 1. (a) Number density (left vertical axis) and flake size in μm^2 (right vertical axis) of the exfoliated multi-layer phosphorene (determined optically) as a function of CCU percentage in ethanol. (b) UV–vis intensity as a function of CCU percentage in ethanol. Inset: spectrum of the viscosity-tuned system showing intensity versus wavelength and the general trend of absorbance at 375 nm.

With this optimized viscosity we find the largest area to be approximately 3 μm^2 whereas the largest previously reported area is around 1 μm^2 [20]. The decrease in flake area for the higher concentrations of CCU, 60% (104 cP) and 80% CCU (190 cP), is likely attributable to a significant decrease in the degree of intercalation. This decrease in the degree of intercalation is possibly related to the steric effects that become important when the CCU concentration is increased, where the amount of bulky CCU molecules creates a barrier against intercalation; this in turn would yield thicker pieces of BP. Additionally, lower-powered sonication, we find, becomes less able to aid in the delamination of the bulk BP due to the high-viscosity (80% CCU system) solvent absorbing the energy imparted into the system.

To further determine the effect of CCU concentration on overall yield, we performed absorption versus wavelength optical spectroscopy, in which the amount of flakes present in each dilution of CCU affects the overall absorption in the ultraviolet-to-visible (UV–vis) portion of the spectrum. As seen

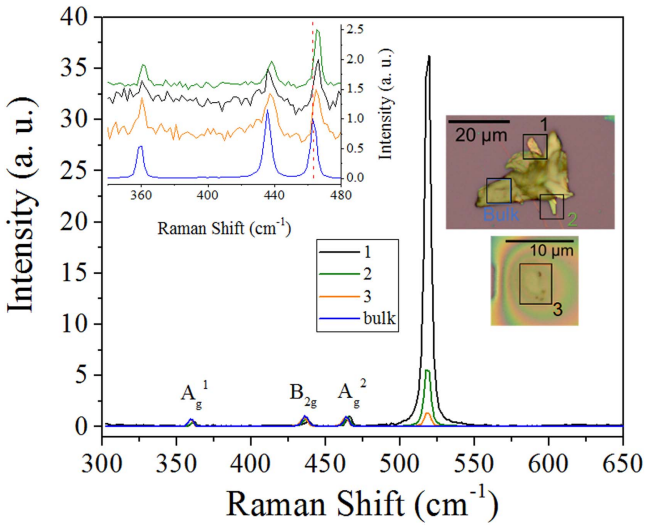

Figure 2. Sample Raman spectra measured for different flake thicknesses generated from a 50% CCU in ethanol mixture. The peaks have been normalized to the A_g^2 mode. Each color (varying flake thickness) corresponds to a highlighted region in the optical images shown in the two right insets (labeled bulk, 1, 2, and 3). Left inset: portions of the Raman spectra showing the A_g^1, B_{2g}, and A_g^2 peaks. The red dashed line is a guide to the eye. Based on this measurement, the thinnest flake achieved is a tri-layer (region '1' in the upper right inset), which is determined from the shift in the A_g^2 peak relative to the bulk.

in figure 1(b), there is minimal absorption from 0% to 40% CCU, however, there is a significant increase from 50% to 60% followed by a subsequent drop in absorption at 80% CCU. This is due to the increase of flakes present in the solution, thus resulting in a greater absorption. Furthermore, the inset to figure 1(b) shows that the absorption at 375 nm has an increased absorbance for the 50% and 60% CCU concentrations, which corroborates the optical inspections of figure 1(a) and suggests that there is either an increase in flake size (50%) or augmented quantity of flakes (60%). This increased absorbance is presumed to be correlated to the total number of flakes present in solution, with a further dependence on the thickness of individual flakes. With larger absorbance, the presence of more flakes is simple to understand, however this increased absorbance can also indicate a larger quantity of thinner, more efficiently absorbing flakes [27, 28].

Figure 2 shows the Raman spectra taken for several different exfoliated flakes with varying thickness. All Raman measurements were carried out under ambient conditions using a 514 nm laser excitation. The A_g^1, B_{2g}, and A_g^2 peaks correspond to the vibrational modes of the BP crystal while the peak at ~519.5 cm^{-1} is due to the SiO_2 substrate [29]. Prior work has shown that the BP layer number can be estimated through the intensity ratio of the A_g^1 and the silicon peak $I_{A_g^1}/I_{Si}$ as well as the shift in the A_g^2 peak with respect to bulk material (it has been suggested that the A_g^2 shift is the most sensitive indicator of the layer number, and that the A_g^2 peak is not noticeably affected by perturbations induced by the underlying substrate) [29, 30]. For the black trace in figure 2, we find $I_{A_g^1}/I_{Si} \sim 0.057$, which would correspond to a flake thickness of $t \sim 0.6$ Å [29]. This thickness corresponds to a single BP layer [8]. However, estimates based upon $I_{A_g^1}/I_{Si}$ are only accurate to within 1–2 nm. We also find an A_g^2 peak shift with respect to bulk of ~1.7 cm^{-1} (highlighted by the dotted red line in the left inset of figure 2), which is consistent with prior Raman measurements of tri-layer BP (when also taking into account the shape of the A_g^2 peak) [30]. Therefore, we conclude that the thinnest BP flake obtained within our experiments is a tri-layer, which is labeled as region 1 in the upper right inset of figure 2.

One of the more intriguing results of this study is flake dimension control with respect to viscosity, as shown in figure 1, where the amount of CCU present in each solution determines the degree of exfoliation. Flake thickness can vary, but overall the thinnest flakes are found to be multilayer (5–10 layers), with the thinnest flake being tri-layer (figure 2), and to have lateral dimensions on the micrometer scale (figure 2 insets). With dilution of the CCU solvent, intercalation happens more readily than in a pure system due to solvation effects of the intercalant molecule on the bulk material. While prior work has demonstrated that higher powered sonication (>100 W) produces thin flakes using a pure, high-viscosity intercalant, we show here that high-powered sonication is not necessary for exfoliation if the species responsible for the exfoliation (in this case CCU) is diluted with a solvent such as ethanol [20, 25]. In fact, high-powered sonication can be detrimental to the overall yield of large-area flakes, due to the sonication breaking down the larger-area flakes into nanosheets of smaller lateral dimensions [16]. Additionally, the high temperatures that result from higher powered sonication are more likely to induce chemical reactions between the solvent system and the BP, rendering them less useful for applications. Furthermore, using a high viscosity straight solvent, such as CCU, introduces the problem of 'purifying' the flakes; due to the high viscosity of the DES, it becomes difficult to remove the CCU successfully without the use of centrifugation. Here, we have successfully replaced centrifugation with a soak in a large excess of the solvent for CCU, e.g. ethanol.

Extending our investigation to the nanoscale scale, we utilize (scanning) transmission electron microscopy ((S)TEM) to generate the micrographs and electron diffraction pattern shown in figure 3. Here, the flakes are observed to be defect-free with only small amounts of oxygen present, which is most likely due to the onset of environmental degradation. From the observed diffraction pattern, we measured lattice d-spacings of 2.63, 2.27, 1.83, 1.37, and 1.16 Å, and we find that the flake structure differed from that of bulk black phosphorus, but the values for the d-spacings closely correlates to the measurements obtained by Brent *et al* in which they measured the d-spacings for few-layer phosphorene [31]. Since the sheets are no longer locked in their bulk arrangement, it is expected that there would be a slight increase to the bond distances and angles in very thin sheets of BP. Figures 3(d) and (e) show the electron energy loss (EEL) spectra of the BP: the latter spectrum indicates that there is no oxidation of the flake of interest in the bulk region (a sharp

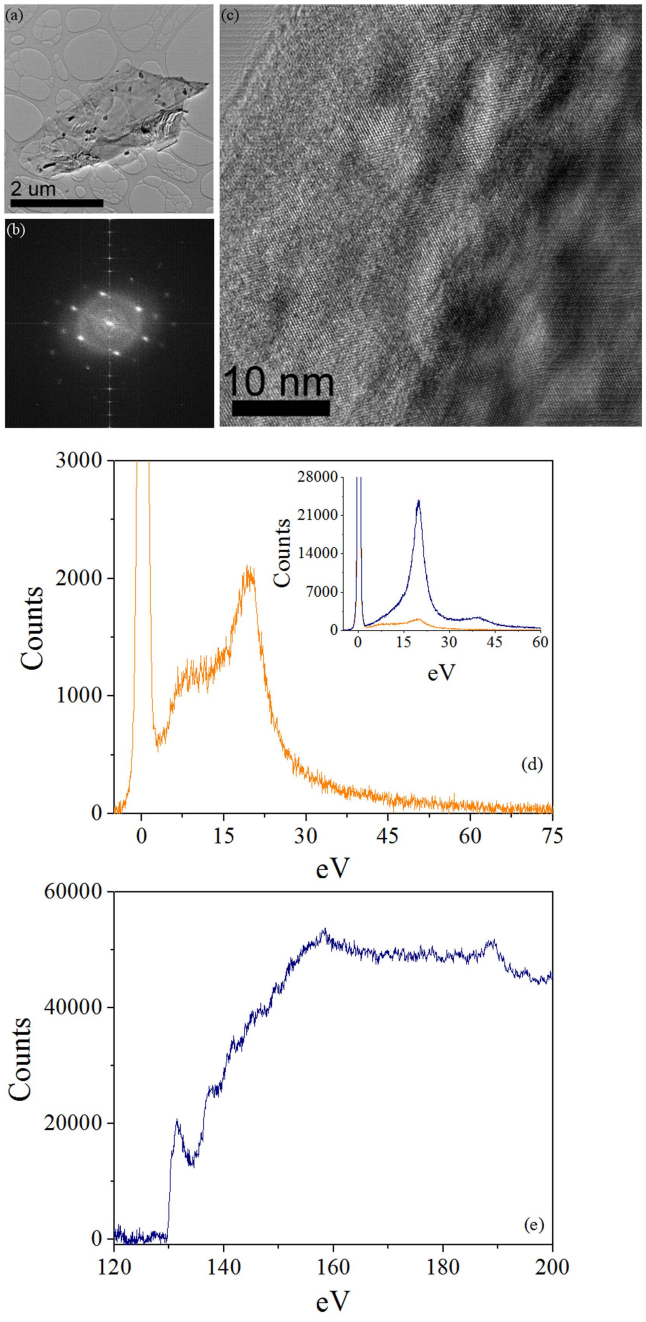

Figure 3. (a) Low magnification transmission electron micrograph of a representative phosphorene flake. (b) FFT and (c) HR-TEM image for the flake shown in (a). (d) Low loss EELS of thin BP. Inset: comparison of the low loss regions for both thin BP (orange) and bulk BP (blue). (e) Core loss of bulk BP showing that phosphorus oxide is not present as was previously demonstrated by Wu *et al* [17].

signal at 130 eV), while the thinner areas of the flake (figure 3(d)), indicate there is a presence of oxidation consistent with the results of Wu *et al* as evident by the presence of a shoulder between 1 and 15 eV in the low loss EELS [32]. figure 3(d) shows the EELS features found on a thin flake, where a comparison between a bulk (blue) and thin region (orange) are displayed in the inset.

Degradation of single and few-layer phosphorene flakes due to environmental exposure is a major concern for device

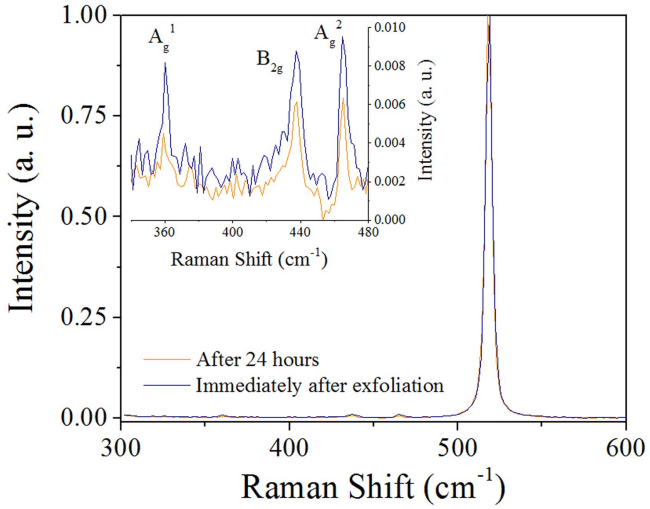

Figure 4. Raman spectra of a BP flake encapsulated within DES taken immediately after exfoliation and 24 h after exfoliation. The spectra have been normalized to the SiO_2 substrate peak intensity. Left inset: portion of the Raman spectra showing the A_g^1, B_{2g}, and A_g^2 peaks. The colors in the inset are the same as in the main figure. The flake of interest is that of figure 2, region/site 3; based on Raman measurements, the BP is less than 5 layers, as evident by the shift in the A_g^2 peak in comparison to the bulk.

applications and represents a significant roadblock that must be overcome in order for phosphorene to be incorporated into future technologies. Prior studies have shown a thickness-dependent degradation of the material due to photoactivated oxidation [30]. This degradation has been observed in time-dependent Raman measurements, which show a nearly complete suppression of the Raman active modes in as little as two hours. Figure 4 shows the results of our time-dependent Raman measurements for an exfoliated BP flake encapsulated within the DES. The observance of the three A_g^1, B_{2g}, and A_g^2 modes 24 h after the initial exfoliation for a BP flake encapsulated within the DES demonstrates the ability of the exfoliating substance to serve as a protective barrier from degradation following the initial exfoliation. We do measure a slight decrease in the three Raman modes after 24 h, and further studies can shed light on the relationship between peak suppression and time (e.g. an exponential dependence). Nevertheless, the data shown in figure 4 demonstrates the ability of the DES to serve as a protective layer for the phosphorene.

4. Conclusion

In conclusion, we demonstrate that a viscosity-tunable solvent system effectively enables the optimized exfoliation of bulk black phosphorus. The ability to generate thin (sub-5 nm) and large flakes (30 μm^2) depends on the medium in which the black phosphorus is sonicated, and our studies show that a 50:50 mixture of CCU to ethanol produces the best results for achieving large, thin flakes, which is highly desirable in preparing phosphorene-based devices. Our flakes are several times larger than what has been previously reported as seen in

both the optical and electron microscopy data. Additionally, the DES system is demonstrated to protect the flakes from environmental degradation over the course of 24 h following the exfoliation. Furthermore, the ability to successfully exfoliate the black phosphorus with a diluted IL or DES, while utilizing less power, offers a more viable technique for black phosphorus and other 2D material production.

Acknowledgments

The authors gratefully acknowledge the members of the technical staff of the Institute for Nanoscience at NRL, Dean R St Amand and Walter A Spratt. We thank Dr Janice Boercker for her assistance with UV–vis data collection. AN performed research courtesy of support from a National Research Council postdoctoral fellowship. This work was supported by the Office of Naval Research: Naval Research Laboratory Basic Research Program. The work at Purdue University is partly supported by NSF under Grant ECCS-1449270, AFOSR/NSF under EFRI 2-DARE Grant EFMA-1433459, and ARO under Grant W911NF-14-1-0572.

References

[1] Geim A K and Novoselov K S 2007 The rise of graphene *Nat. Mater.* **6** 183–91
[2] Caldwell J D and Novoselov K S 2015 Mid-infrared nanophotonics *Nat. Mater.* **14** 363–6
[3] Jiang X F, Weng Q H, Wang X B, Li X, Zhang J, Golberg D and Bando Y 2015 Recent progress on fabrications and applications of boron nitride nanomaterials: a review *J. Mater. Sci. Technol.* **31** 589–98
[4] Chhowalla M, Liu Z and Zhang H 2015 Two-dimensional transition metal dichalcogenide (TMD) nanosheets *Chem. Soc. Rev.* **44** 2584–6
[5] Radisavljevic B and Kis A 2013 Mobility engineering and a metal–insulator transition in monolayer MoS_2 *Nat. Mater.* **12** 815–20
[6] Pinchuk I V, Odenthal P M, Ahmed A S, Amamou W, Goldberger J E and Kawakami R K 2014 Epitaxial co-deposition growth of $CaGe_2$ films by molecular beam epitaxy for large area germanane *J. Mater. Res.* **29** 410–6
[7] Liu H, Neal A T, Zhu Z, Luo Z, Xu X F, Tomanek D and Ye P D 2014 Phosphorene: an unexplored 2D semiconductor with a high hole mobility *ACS Nano* **8** 4033–41
[8] Li L K, Yu Y J, Ye G J, Ge Q Q, Ou X D, Wu H, Feng D L, Chen X H and Zhang Y B 2014 Black phosphorus field-effect transistors *Nat. Nanotechnol.* **9** 372–7
[9] Guo Z N *et al* 2015 From black phosphorus to phosphorene: basic solvent exfoliation, evolution of raman scattering, and applications to ultrafast photonics *Adv. Func. Mater.* **25** 6996–7002
[10] Kou L, Chen C and Smith S C 2015 Phosphorene: fabrication, properties, and applications *J. Phys. Chem. Lett.* **6** 2794–805
[11] Wang F, Stepanov P, Gray M, Lau C N, Itkis M E and Haddon R C 2015 Ionic liquid gating of suspended MoS_2 field effect transistor devices *Nano Lett.* **15** 5284–8
[12] Uesugi E, Goto H, Eguchi R, Fujiwara A and Kubozono Y 2013 Electric double-layer capacitance between an ionic liquid and few-layer graphene *Sci. Rep.* **3** 1595
[13] Kamalakar M V, Madhushankar B N, Dankert A and Dash S P 2015 Effect of high-k dielectric and ionic liquid gate on nanolayer black-phosphorus field effect transistors *Appl. Phys. Lett.* **107** 113103
[14] Saito Y and Iwasa Y 2015 Ambipolar insulator-to-metal transition in black phosphorus by ionic-liquid gating *ACS Nano* **9** 3192–8
[15] Nuvoli D, Valentini L, Alzari V, Scognamillo S, Bon S B, Piccinini M, Illescas J and Mariani A 2011 High concentration few-layer graphene sheets obtained by liquid phase exfoliation of graphite in ionic liquid *J. Mater. Chem.* **21** 3428
[16] Hanlon D *et al* 2015 Liquid exfoliation of solvent-stabilized few-layer black phosphorus for applications beyond electronics *Nat. Commun.* **6** 8563
[17] Kang J, Wood J D, Wells S A, Lee J H, Liu X L, Chen K S and Hersam M C 2015 Solvent exfoliation of electronic-grade, two-dimensional black phosphorus *ACS Nano* **9** 3596–604
[18] Sutto T E, Duncan T T and Wong T C 2009 X-ray diffraction studies of electrochemical graphite intercalation compounds of ionic liquids *Electrochim. Acta* **54** 5648–55
[19] Sutto T E and Duncan T T 2012 The intercalation behavior of ionic liquids in the layered metal dichalcogenide TiS_2 *Electrochim. Acta* **77** 204–11
[20] Zhao W C, Xue Z M, Wang J F, Jiang J Y, Zhao X H and Mu T C 2015 Large-scale, highly efficient, and green liquid-exfoliation of black phosphorus in ionic liquids *ACS Appl. Mater. Inter.* **7** 27608–12
[21] Gu C, Zhang H, Wang X and Tu J 2013 Synthesis of reduced graphene oxide by an ionothermal method and electrochemical performance *RSC Adv.* **3** 11807–15
[22] Acik M, Dreyer D R, Bielawski C W and Chabal Y J 2012 Impact of ionic liquids on the exfoliation of graphite oxide *J. Phys. Chem.* C **116** 7867–73
[23] Abbott A P, Capper G, Davies D L, Rasheed R K and Tambyrajah V 2003 Novel solvent properties of choline chloride/urea mixtures *Chem. Commun.* **1** 70–1
[24] Cheng K H, Jacobson A J and Whittingham M S 1981 Hexagonal tungsten trioxide and its intercalation chemistry *Solid State Ion.* **5** 355–8
[25] Ludwig T *et al* 2015 Mechanism of bismuth telluride exfoliation in an ionic liquid solvent *Langmuir* **31** 3644–52
[26] Sresht V, Padua A A H and Blankschtein D 2015 Liquid-phase exfoliation of phosphorene: design rules from molecular dynamics simulations *ACS Nano* **9** 8255
[27] Woomer A H, Farnsworth T W, Hu J, Wells R A, Donley C L and Warren S C 2015 Phosphorene: synthesis, scale-up, and quantitative optical spectroscopy *ACS Nano* **9** 8869–84
[28] Nair R R, Blake P, Grigorenko A N, Novoselov K S, Booth T J, Stauber T, Peres N M R and Geim A K 2008 Fine structure constant defines visual transparency of graphene *Science* **320** 1308–1308
[29] Castellanos-Gomez A *et al* 2014 Isolation and characterization of few-layer black phosphorus *2D Mater.* **1** 025001
[30] Favron A, Gaufres E, Fossard F, Phaneuf-L'Heureux A L, Tang N Y W, Levesque P L, Loiseau A, Leonelli R, Francoeur S and Martel R 2015 Photooxidation and quantum confinement effects in exfoliated black phosphorus *Nat. Mater.* **14** 826–33
[31] Brent J R, Savjani N, Lewis E A, Haigh S J, Lewis D J and O'Brien P 2014 Production of few-layer phosphorene by liquid exfoliation of black phosphorus *Chem. Commun.* **50** 13338–41
[32] Wu R J, Topsakal M, Low T, Robbins M C, Haratipour N, Jeong J S, Wentzcovitch R M, Koester S J and Mkhoyan K A 2015 Atomic and electronic structure of exfoliated black phosphorus *J. Vac. Sci. Technol.* A **33** 060604